Proc. of SPIE Vol. 0288, Los Alamos Conference on Optics '81, ed. D.H. Lienbenberg (Jan 1981) Copyright SPIE

Mirror figure-of-merit and material index-of-goodness for high power laser beam reflectors

Claude A. Klein
Research Division, Raytheon Company
Waltham, Massachusetts 02254

Abstract

The purpose of this paper is to provide guidelines for assessing the performance of actively cooled high-power/high-energy laser beam (HEL) reflectors. The first segment concerns a highly simplified situation involving steady-state irradiance-mapping distortions only; a comprehensive "mirror figure of merit" may thus be defined for characterizing the performance of HEL reflectors, in the absence of pressure-induced ripples. In the second part, a generalized mirror/heat-exchanger model is used for evaluating the potential impact of coolant-induced distortions, for identifying key properties of mirror materials, and for creating a "material index of goodness" applicable to HEL reflectors; the most promising candidates are silicon carbide and tungsten.

1. Introduction

The development of high-energy laser (HEL) systems has stimulated a great deal of activity relating to the physics and the technology of optical components designed for handling high-power beams of infrared light (see, for instance, Ref. 1). The reason for this is that typical HEL systems involve an optical train consisting of ten or more mirrors, which must be capable of transporting and directing the laser beam without seriously degrading the optical quality of the system. In this paper, we address the problem of evaluating mirror-design features and mirror-material parameters that affect phase aberrations and, hence, control the performance of HEL systems with regard to both focal intensities and on-target fluences; related topics such as "catastrophic" failure modes associated with thermally induced stresses or temperature excursions are beyond the scope of the present investigation since they are of peripheral importance in selecting mirror-substrate materials.

Currently operational beam-relay/beam-steering mirrors consist of a thin, highly reflecting faceplate, which transfers to a coolant fluid the fractional laser energy that is deposited at the surface, and which is stiffly held to a stable backup structure that minimizes thermo-mechanical deformation modes. The finite thermal conductivity of the substrate material causes temperature gradients to develop: Radial gradients, which deform the faceplate surface, and axial gradients, which may alter the mirror curvature. Thermally induced surface deformations resulting from spatial variations in beam intensity generate "irradiance-mapping" wavefront distortions and have been the subject of previous investigations.[2] Mirror "bowing" involves low-spatial-frequency deformations, which are usually modelled as spherical aberrations[3]; following Holt,[4] we will assume that they can be compensated for by means of refocussing procedures and, thus, can be ignored in the context of assessing the performance of HEL mirror substrates. This, however, does not apply to deformations of the faceplate resulting from the flow of pressurized coolant, unless they can be reduced to a negligible amount or *de facto* eliminated by figuring the mirror surface under a static pressure distribution that simulates the actual operating pressures of the heat exchanger.

The performance of a mirror-substrate material is best characterized on the basis of its ability to minimize wavefront errors induced by dynamic loading conditions. In this context, we recall that, for small aberrations, the reduction in far-field intensity obeys the Strehl approximation,[5]

$$i = 1-(2\pi/\lambda)^2(\overline{OPD})^2 , \tag{1}$$

where $\overline{OPD}$ represents a properly evaluated optical path difference, which is twice the RMS variation of the mirror-surface displacement, that is, $\overline{OPD} = 2\Delta$ at normal incidence.* The RMS surface distortion Δ includes initial figuring errors as well as high-spatial-frequency deformations caused by the incident beam ($\delta\ell_I$) and the pressurized coolant ($\delta\ell_P$). The mechanisms involved are uncorrelated, which means that the mirror distortion, as expressed in terms of an RMS number, is given by

$$\Delta = \sqrt{(\bar{\tau}_f)^2+(\bar{\delta}_I)^2+(\bar{\delta}_P)^2} . \tag{2}$$

Note that the symbol $\bar{\delta}$ is defined as follows:

$$\bar{\delta} = [\langle\delta\ell(x,y)^2\rangle - \langle\delta\ell(x,y)\rangle^2]^{\frac{1}{2}} , \tag{3}$$

where the brackets refer to intensity-weighted area averages. *Pour fixer les idées,* consider a HEL mirror operating at HF/DF laser wavelengths; based on the Maréchal criterion for allowable optical distortions

* *The symbols are as identified in the Appendix.*

($i \lesssim 0.80$), the tolerable surface distortion must be smaller than 120 nm (or less than five microinches), which brings forth the level of physical stability that must be achieved in a HEL environment.

At this time, unalloyed molybdenum is usually chosen for fabricating HEL mirror faceplates and heat exchangers; this is because molybdenum exhibits a combination of several desirable physical properties such as low expansion coefficient (α), high thermal conductivity (K), and favorable elastic modulus (E) in conjunction with relative ease of machining and polishing. Other metals of merit in the high-power mirror technology area include copper and tungsten,[6] but it should be recognized that "new" substrate materials such as carbon/carbon, silicon, and silicon carbide may improve the performance of HEL reflectors if and when suitable fabrication methods become known. Values of α, K, and E for mirror-substrate materials of current interest are listed in Table 1.

Table 1. Key properties of HEL mirror-substrate material candidates. Data for Cu, Mo, W, C/C, and Si are as listed in Ref. 4. Data for SiC are as specified for hot-pressed silicon carbide (CERALLOY 146I) manufactured by Ceradyne, Inc., Santa Ana (92705).

Substrate Material	Expansion Coefficient ($10^{-6}K^{-1}$)	Thermal Conductivity (W $cm^{-1}K^{-1}$)	Young's Modulus (10^6 psi)
Copper	15	3.8	16
Molybdenum	5.0	1.4	47
Tungsten	4.8	1.8	60
Carbon/Carbon	1.3	1.5	1.0
Silicon	2.6	1.5	16
Silicon Carbide	4.5	1.6	60

The primary purpose of this paper is to provide analytical insights in developing guidelines for assessing the performance of water-cooled laser beam reflectors. In this context, I will first consider a highly simplified situation involving irradiance-mapping distortions only and derive equations that relate local surface displacements to the incident beam-power density, in a CW mode (Sec. 2). A comprehensive "mirror figure of merit" may thus be defined for characterizing the behavior of HEL reflectors in the absence of pressure ripples (Sec. 3). In Sec. 4, I will make use of Holt's generalized mirror/heat-exchanger model[4] in order to specify how heat-transfer coefficients relate to critical design features and show how coolant-flow conditions may create distortions that match thermally induced effects. In this light, key mirror-substrate material parameters can be identified and combined into a "material index of goodness" that should be applicable to a wide range of situations (Sec. 5). Our conclusions are stated in Sec. 6.

2. Simple mirror model

Figure 1 illustrates the design concept currently implemented in manufacturing actively cooled high-power laser light reflectors. The mirror faceplate is typically 1-mm thick and is subjected to thermal loadings owing to unavoidable absorption of some of the incident radiation. Heat that is deposited at the front surface must be efficiently removed before it causes potentially damaging thermal stresses and seriously deforms the mirror faceplate; this is the function of the heat exchanger with its array of cooling channels, which are mounted on a backup structure designed to provide a stable, highly rigid base for the complete assembly. The "simple mirror model," as originally formulated by Sparks,[7] makes three important assumptions:

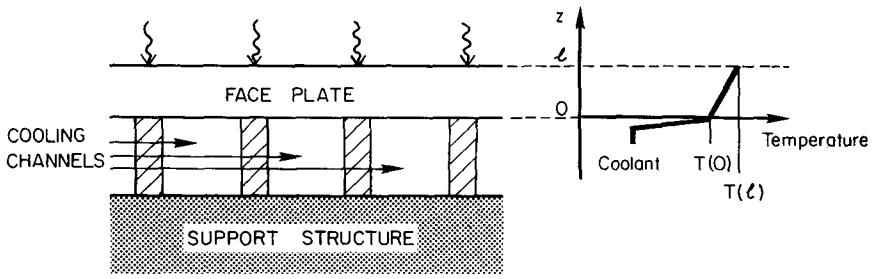

Figure 1. Simple HEL mirror/heat-exchanger model.

(a) Radial heat diffusion can be neglected, which presumes that the thickness ℓ of the faceplate is small relative to the scale of spatial variations in beam intensity.

(b) The backside of the faceplate interfaces with the coolant fluid to ensure an adequate level of heat transfer but can be maintained in its original plane ($z = 0$).

(c) Out-of-plane growth of the mirror front surface only occurs as a result of beam impingement and maps the incident irradiance pattern; in this sense, the simple mirror model provides a vehicle for investigating mirror-related "thermal lensing" phenomena and, thus, for assessing the impact of substrate-material properties on irradiance-mapping mirror distortions.

If a laser beam of intensity I(x,y) impinges on a mirror surface of absorptance A_M, there is a constant flow of heat, $A_M I$, into the substrate. If, in addition, we postulate that the rear surface can be maintained at a constant temperature T(O), the steady-state* temperature distribution through the faceplate becomes a linear function of position[8]:

$$T(z)-T(O) = (A_M I/K)z. \tag{4}$$

In equilibrium, the temperature of the back surface, measured with respect to the temperature of the coolant, levels off at

$$T(O) = A_M I/h \tag{5}$$

thus indicating that laser irradiance results in a temperature increase

$$\delta T(z) = A_M I(1/h + z/K) \tag{6}$$

(see Fig. 1); in other words, the axial temperature profile is made up of a temperature gradient across the faceplate, which reflects the thermal conductivity of the substrate, and a temperature drop across the boundary layer, which is controlled by the heat-transfer coefficient.

If deformations of the back surface of the mirror faceplate can be effectively suppressed, any expansion of the faceplate caused by temperature increments $\delta T(z)$ manifests itself through out-of-plane growth of the front surface. This growth stems from a single integration,

$$\delta \ell_I = \int_o^\ell \varepsilon_z(z)dz \ , \tag{7a}$$

where $\varepsilon_z(z)$ is the differential strain for axial expansion and includes stress-related contributions in accord with Hooke's law.[9] For axisymmetric loadings, for instance, we have

$$\varepsilon_z(z) = \alpha\delta T(z) + (1/E)[\sigma_z - \nu(\sigma_\rho + \sigma_\theta)] \ , \tag{8a}$$

the sigmas representing principal stress components. Thermally induced stresses are difficult to evaluate in a situation as applies here, where the temperature is a function of both axial and radial coordinates; in the present case, however, thin-plate theory may provide good estimates because the thickness of the faceplate ($\ell \lesssim 0.1$ cm) should be much smaller than the diameter of the mirror ($D \gtrsim 10$ cm). In other words, the faceplate should be subjected to minimal axial stresses, and since

$$\sigma_\rho = \alpha E[(1/R^2)\int_o^R \delta T \ rdr - (1/r^2) \int_o^r \delta T \ rdr] \tag{9a}$$

$$\sigma_\theta = \alpha E[(1/R^2)\int_o^R \delta T \ rdr + (1/r^2) \int_o^r \delta T \ rdr - \delta T] \ , \tag{9b}$$

we take it that the differential strain is simply

$$\varepsilon_z(z) = \alpha(1+\nu)\delta T(z) - \alpha\nu\langle\delta T(z)\rangle \ , \tag{8b}$$

where $\langle\delta T(z)\rangle$ refers to a conventionally averaged temperature over the mirror area. It follows that a straightforward integration as in (7a), with $\delta T(z)$ as in (6), yields

$$\delta \ell_I = A_M(\ell/h + \ell^2/2K)[\alpha(1+\nu)I - \alpha\nu\langle I\rangle] \ , \tag{7b}$$

which clearly demonstrates that the faceplate surface deformation "images" or "maps" the spatial variations of the incident beam.

3. Mirror figure of merit

Equation (7b) includes a term proportional to $\langle I\rangle$, which does not contribute to the variance of the optical path difference; as defined earlier, the thermally induced surface distortion then amounts to

$$\overline{\delta_I} = \alpha(1+\nu)(\ell/h + \ell^2/2K)A_M\bar{I} \ , \tag{10a}$$

where $\bar{I}$ is the RMS variation in beam intensity across the mirror faceplate. In this simple model, the surface distortion increases linearly with the RMS intensity $\bar{I}$, the "slope" involving a combination of material parameters and design features that can serve as a measure of the performance of the reflector:

---

* *Note that the characteristic thermal response time of the faceplate is* $\tau = (4/\pi^2)\ell^2/\kappa$, *which would indicate that a 1-mm thick molybdenum faceplate with a diffusivity* κ *of 0.55* $cm^2 sec^{-1}$ *should reach thermal equilibrium in less than 100 msec.*

$$\bar{\delta}_I = (1/FoM_M)\bar{I} \ . \tag{10b}$$

In this manner, I am introducing the concept of a "mirror figure of merit," which is best expressed as follows*:

$$FoM_M = K'/(A_M \cdot \xi). \tag{11}$$

The factor K' characterizes the efficiency of the entire heat-transfer process from the mirror surface to the coolant fluid, *à savoir*,

$$K' = \frac{2K/\ell^2}{1+(2/Nu)} \tag{12}$$

if we make use of the Nusselt number $Nu = \ell h/K$. The factor A_M, of course, refers to the mirror absorptance, whereas ξ describes the stress-augmented expansion of the faceplate material,

$$\xi = \alpha(1+\nu), \tag{13}$$

and, thus, plays the same role as the distortion coefficient χ of HEL windows. We may also note that the figure of merit FoM_M is in units of watts per square centimeter per centimeter, which points to a straightforward interpretation in the sense that $1/FoM_M$ measures the growth of the mirror surface per unit incident power density.

Equation (12) clearly specifies how the figure of merit of actively cooled mirrors will be affected by the quality of the heat exchanger. If the cooling is very efficient, that is, if Nu >> 2, the figure of merit becomes

$$FoM_M = \frac{2K/\ell^2}{A_M \cdot \xi} \tag{14a}$$

thus emphasizing that thermal diffusion across the faceplate becomes a critical parameter; if, on the contrary, the Nusselt number remains much smaller than two (poor cooling!), the figure of merit no longer includes the thermal conductivity, the heat-transfer coefficient being the limiting factor:

$$FoM_M = \frac{h/\ell}{A_M \cdot \xi} \ . \tag{14b}$$

In this regard, we note that, currently, heat-transfer coefficients of 10 $W/(cm^2K)$ can be achieved with 20-mil (0.51-mm) thick molybdenum faceplates polished under pressure,[7] which points to Nusselt numbers of no more than 0.35, thus demonstrating that state-of-the-art water-cooled mirror/heat-exchangers are far from having reached a desirable level of performance.[11]

Table 2. Figure of merit, irradiance-mapping factor, and surface-temperature increase of "simple" HEL mirrors; material properties are as listed in Table 1 with Poisson ratios always assumed equal to 0.30.

Substrate Material	CASE 1(a)			CASE 2(b)		
	FoM_M (MW/cm^3)	$\bar{\delta}_I/\bar{I}$ $Å/(W\ cm^{-2})$	δT(c) (K)	FoM_M (GW/cm^3)	$\bar{\delta}_I/\bar{I}$ $mÅ/(W\ cm^{-2})$	δT(c) (K)
Copper	10.2	9.76	50.1	9.6	10.40	0.113
Molybdenum	30.6	3.26	50.3	26.1	3.83	0.136
Tungsten	32.0	3.12	50.3	28.1	3.56	0.128
Carbon/Carbon	117.9	0.85	50.3	101.0	0.99	0.133
Silicon	59.0	1.69	50.3	50.7	1.97	0.133
Silicon Carbide	34.1	2.93	50.3	29.6	3.38	0.131

(a) *Early designs:* $A_M = .005$, $h = .1\ W\ cm^{-2}K^{-1}$, $\ell = .1$ *cm.*
(b) *Advanced designs:* $A_M = .001$, $h = 10\ W\ cm^{-2}K^{-1}$, $\ell = .05$ *cm.*
(c) *At an irradiance level of 1* kW/cm^2.

* *In this connection, we may emphasize that the figure of merit* FoM_M *characterizes mirror-induced wavefront errors in a formally identical manner as window figures of merit describe thermal lensing phenomena in HEL windows:* $FoM_W = C'/(A_W \cdot \chi)$, *where C' is the specific heat per unit volume,* A_W *is the absorptance of the window, and* χ *is an appropriate optical distortion coefficient (see Ref. 10).*

Multi-layer dielectric coatings are usually required to enhance the reflectivity of high-power laser mirrors at the wavelengths of interest; it is therefore the coating that determines the magnitude of the absorptance A_M. For this reason, and since Poisson's ratio does not affect the distortion coefficient ξ in a significant way, we conclude that the thermal expansion coefficient of the substrate represents the single most important material parameter if irradiance mapping is the only source of dynamic surface distortion. In Table 2, there are some figures of merit for HEL reflectors having substrates made of the materials listed in Table 1. "Early designs" are based on coating absorptances, heat-transfer coefficients, and faceplate thicknesses representative of, say, ten-year old technology; it is seen that molybdenum, tungsten, and silicon carbide behave very similarly in the sense that out-of-plane growth amounts to about 3 Å/(W cm^{-2}), in good agreement with typical measured values for small-diameter mirrors.[12] "Advanced designs" with coating absorptances as low as 0.1%[1] should give rise to irradiance-mapping distortions almost three orders of magnitude lower; in effect, the current state of the art ($\lambda/20$ at 10.6 μm for incident flux densities in excess of 150 kW/cm^2)[6] already may approach this level of performance. Finally, we note that these advanced mirrors operate at dramatically lowered temperatures, the surface-temperature rise,

$$\delta T(\ell) = A_M I(1/h + \ell/K). \tag{15}$$

remaining very reasonable even at irradiances in the multi-kilowatt per square centimeter range.

4. Generalized mirror model

I mentioned earlier (see Sec. 1), that Holt[4] had developed a "generalized mirror model" in order to provide a sounder base for evaluating water-cooled HEL beam reflectors; more specifically, for relating both irradiance- and pressure-induced distortions to the mirror configuration, the material properties, and the coolant flow. The configuration is shown in Fig. 2 and requires only two geometrical parameters for a complete description: the characteristic thickness-dimension ℓ and the coolant path-length L. Note that the model involves a secondary heat exchanger, which isolates the support structure from the heated primary loop and, thus, minimizes power-dependent thermal deformations of the mirror assembly.

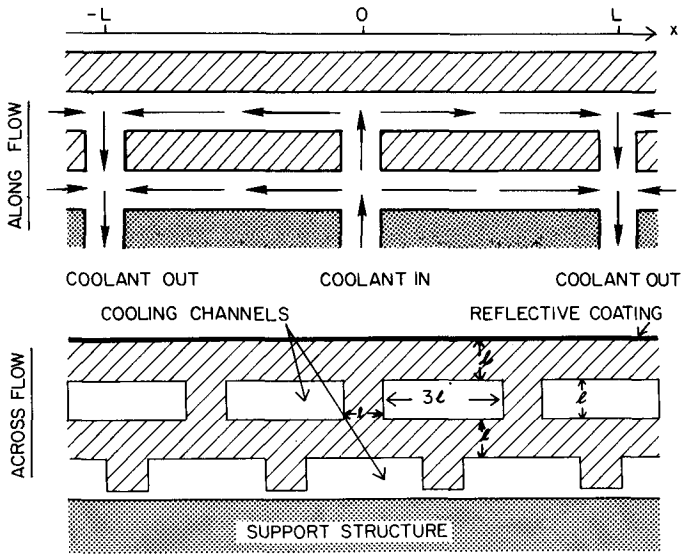

Figure 2. Generalized mirror/heat-exchanger model as proposed by Holt (Ref. 4).

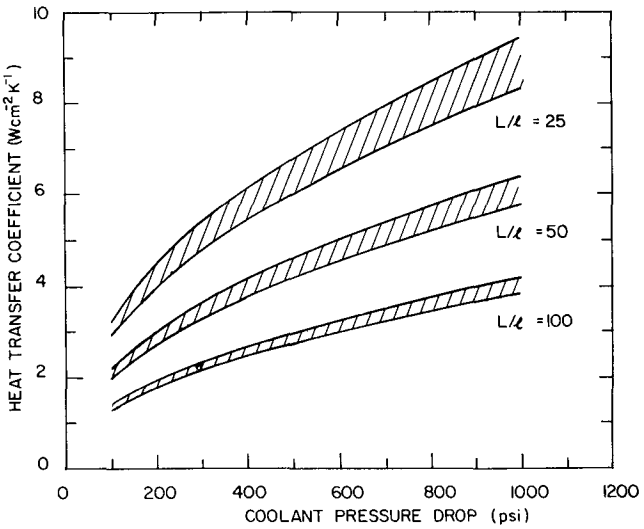

Figure 3. Calculated heat-transfer coefficients for characteristic thicknesses ranging from 10 to 50 mil (0.025 to 0.125 mm).

Returning now to Eq. (10a), we know already that irradiance-mapping distortions should obey an equation such as

$$\bar{\delta}_I \simeq \alpha(\ell/h_{eff} + \ell^2/2K)A_M\bar{I} \tag{16}$$

if h_{eff} represents an effective heat-transfer coefficient. This coefficient is made up of two contributions, a contribution reflecting the removal of heat by the coolant and a contribution due to heat pickup from the coolant, which add up as follows:

$$1/h_{eff} = 1/h_1 + 1/h_2 . \tag{17}$$

Assuming turbulent water flow, Holt[4] derives semi-empirical expressions, which amount to stating that

$$\frac{1}{h_1} = \frac{(.900)(L^{.46})}{(\ell^{.37})(P^{.46})} \tag{18a}$$

and

$$\frac{1}{h_2} = \frac{(8.64 \times 10^{-4})(L^{1.57})}{(\ell^{1.71})(P^{.57})} \tag{18b}$$

if the coolant pressure drop P is in psi. Effective heat-transfer coefficients obtained on this basis are shown in Fig. 3 and take on values that are indeed representative of current heat-exchanger technology ($1 \lesssim h_{eff} \lesssim 10$ W cm^{-2}K^{-1}). Note that it is the ratio of flow path-length and characteristic axial dimension in addition to the coolant pressure drop that determine the efficiency of the cooling process. Because of the complexities involved in augmenting the differential pressure per unit length of flow passage, we conclude that values of h_{eff} that exceed 10 W/(cm^{2}K) are well beyond the state of the art of water-cooled mirror technology.

The distortion caused by the flow of coolant normally originates from bending and shear deformations induced by the pressure acting in the cooling channels but may also include a thermal component associated with frictional heating that "scales" with pressure. In the light of Holt's analysis,[4] it would appear that, averaged in the direction normal to the flow, the coolant-induced surface deflection at station $\underline{x}$ (see Fig. 2) is

$$\delta\ell_p(x) = P\ell[(19.7/E)(1-|x/L|) + .0107\alpha|x/L|] , \tag{19}$$

which reflects the observation that pressure-induced deflections peak at the coolant inlet ($x = 0$), whereas frictional heating peaks at the outlet ($x = \pm L$). The RMS distortion, therefore, amounts to

$$\bar{\delta}_p = P\ell[(\bar{x}/L)|(19.7/E)-.0107\alpha|] \tag{20a}$$

and since, in a first approximation, we have

$$\bar{x} = [(1/L)\int_0^L x^2 dx-(L/2)^2]^{\frac{1}{2}} = L/2\sqrt{3} , \tag{21}$$

we arrive at the following estimate:

$$\bar{\delta}_p = (.289)P\ell[(19.7/E)-.0107\alpha] , \tag{20b}$$

which indicates that the behavior of the mirror with regard to "pressure mapping" should be a strong function of the substrate's modulus of elasticity.

For the purpose of assessing the relative weight of beam-induced and coolant-induced distortions in the context of this generalized mirror model, I now propose to examine the behavior of a "hypothetical" HEL mirror whose substrate properties are those of an "average" mirror-material candidate in terms of the data listed in Table 1. In other words, I will use the following values for the expansion coefficient, the thermal conductivity, and the elastic modulus: $\alpha = 5.5 \times 10^{-6}$K^{-1}, K = 1.9 W cm^{-1}K^{-1}, and E = 33 × 10^6 psi, which are not too different from those of the molybdenum standard. Other key features of this mirror (coating absorptance, characteristic dimension, flow path length) are given in Fig. 4, which portrays the situation as a function of

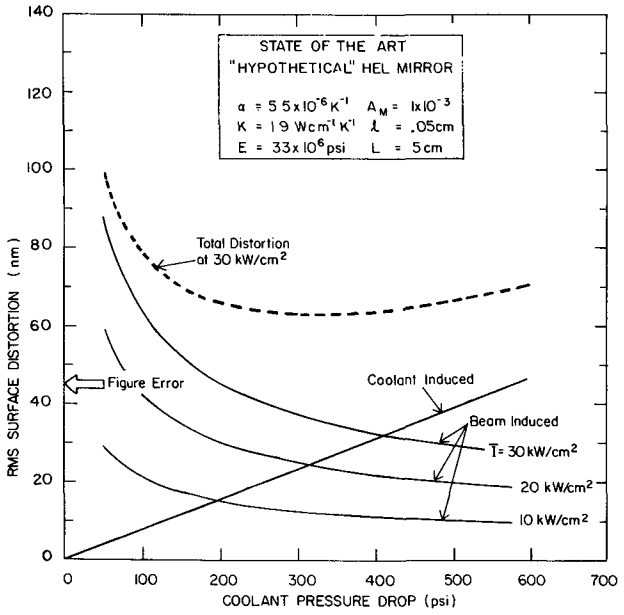

Figure 4. Surface-distortion analysis for a water-cooled laser mirror.

the coolant pressure drop; evidently, given a level of incident irradiance, there is a range of acceptable coolant pressures, beyond which the performance of the system again deteriorates. For example, according to Fig. 4, the total distortion Δ [see Eq. (2)] at an incident RMS irradiance of 30 kW/cm^2 should not exceed 65 nm, for coolant pressures of 300 to 400 psi. This calculation assumes an initial figuring error of 45 nm, which is indicative of a $\lambda_{vis}/10$ error typical of large-diameter optics. For completeness, and since RMS variations in beam intensity essentially reflect the average power density, we may point out that the situation described in Fig. 4 applies to laser beams of 1 to 3 MW having effective diameters of about 10 cm.

5. Material index of goodness

The objective of this section is to examine how substrate material properties relate to, or control, the performance of generalized mirrors. Keeping in mind that the surface absorptance is entirely determined by the quality of the coating, an appropriate expression for beam-induced distortions immediately derives from Eq. (16):

$$\bar{\delta}_I/\ell \propto \alpha(1/h_{eff} + \ell/2K), \tag{22}$$

which confirms that the linear coefficient of thermal expansion is the "driving" factor. Furthermore, Fig. 5 demonstrates that, for realistic values of the heat-transfer coefficient and the faceplate thickness, an increase in thermal conductivity beyond, say, 1 W cm^{-1}K^{-1} makes little difference; in other words, since presently contemplated mirror-substrate materials (see Table 1) are all in the K $\gtrsim$ 1 W cm^{-1}K^{-1} class, it appears that thermal conductivity is an essentially irrelevant parameter from the point of view of rating HEL mirror-material candidates.

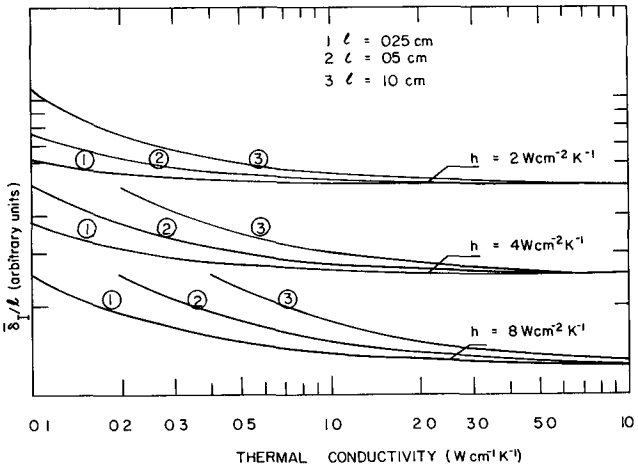

Figure 5. Examines how the thermal conductivity of the substrate affects beam-induced distortions.

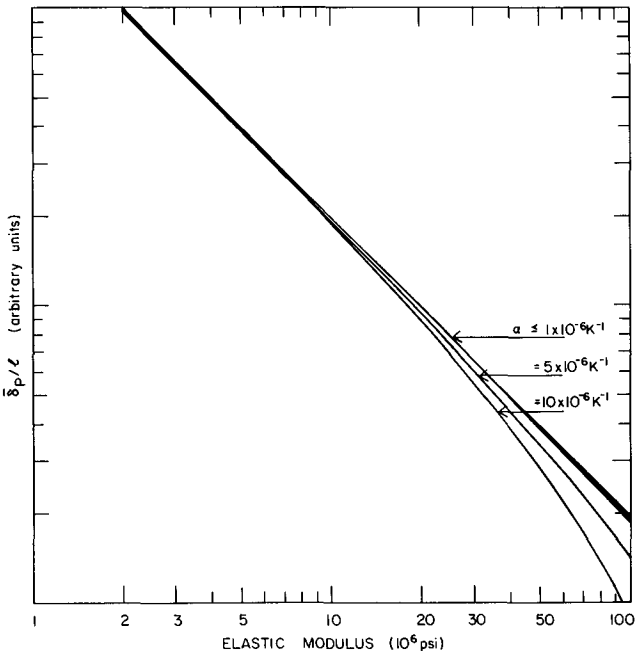

Figure 6. Examines how the expansion coefficient of the substrate affects coolant-induced distortions.

Similarly, for coolant-induced distortions we may write

$$\bar{\delta}_p/\ell \propto (19.7/E) - .107\,\alpha \tag{23}$$

and examine whether thermal expansion has a significant effect. Figure 6 demonstrates that the effect is minimal even in dealing with high-stiffness materials. For this reason, we conclude that the modulus of elasticity is the only other material parameter to be considered if the situation requires that pressure-related deformations be minimized.

Guidelines for selecting the "best" mirror-material candidate thus emerge in a straightforward manner: The coefficient of thermal expansion, α, should be small enough to reduce beam-induced distortions, and the modulus of elasticity, E, must be large enough to minimize coolant-induced deformations. In this light, it follows that a simple combination of these two material parameters can provide an appropriate index of goodness,

$$\text{IoG} = E/\alpha\,, \tag{24}$$

which should be maximized to achieve optimum performances whenever the generalized-mirror-model description applies; Table 3 shows how our candidates rate in terms of this index. If indeed these numbers provide dependable guidelines, it would appear that (a) Silicon carbide and tungsten are the two leading candidates, primarily because of their superior stiffness; (b) Silicon does not have the potential to afford an improvement over molybdenum; and (c) A material such as carbon/carbon with its very low modulus becomes just as undesirable as copper, which is handicapped by its high expansion coefficient.

Table 3. Index of goodness for HEL mirror-substrate material candidates.

Substrate Material	IoG (10^{12} psi·K)	IoG (relative to Mo)	Rank
Copper	1.07	0.11	5
Molybdenum	9.40	1.00	3
Tungsten	12.50	1.33	2
Carbon/Carbon	0.77	0.08	6
Silicon	6.15	0.65	4
Silicon Carbide	13.33	1.42	1

6. Conclusions

● There is no universal figure of merit for assessing the ability of mirror materials to minimize load-induced distortions occurring in conjunction with the operation of high-power laser beam reflectors. The "figure of merit" derived in Sec. 3, $FoM_M = K'/(A_M \cdot \xi)$, characterizes the response of actively cooled mirrors in the context of a highly simplified irradiance-mapping-distortions-only approach. This analysis emphasizes the potential of low-expansion/zero-expansion substrates such as carbon/carbon composites but appears to be misleading because it disregards the importance of adequate mechanical properties.

● An "index of goodness" as proposed in Sec. 5, $IoG = E/\alpha$, reflects the observation that coolant-pressure related considerations dictate a high modulus of elasticity. This index, however, does not account for possible deficiencies in dimensional stability triggered by thermal cycling. Additional sets of material parameters are required for a full description of such aspects of mirror technology.

● In principle, silicon carbide and tungsten are more desirable mirror-substrate materials than molybdenum. Silicon carbide, in particular, is attracting increasing attention because it can be polished exceedingly well.[13] As methods and procedures for fabricating suitable structures progress, we may anticipate that the availability of these materials will lead to significant improvements in HEL mirror performance.

Appendix

A_M : Mirror absorptance
E : Elastic modulus
h : Heat-transfer coefficient
i : Strehl ratio
I : Beam intensity
K : Thermal conductivity
ℓ : Faceplate thickness
L : Flow path length
Nu : Nusselt number
P : Coolant pressure drop
r : Radial coordinate
R : Mirror radius
T : Faceplate temperature
x,y : Cartesian coordinates
z : Axial coordinate

α : Expansion coefficient
δ_I : Beam-induced distortion (RMS)
δ_p : Cooland-induced distortion (RMS)
$\delta\ell$: Local surface deflection
δT : Temperature increase
Δ : Total surface distortion
ε_z : Axial strain
κ : Thermal diffusivity
λ : Laser wavelength
ν : Poisson's ratio
ξ : Mirror distortion coefficient
σ_i : Principal stress component
τ : Thermal response time
τ_f : Figuring error (RMS)
χ : Window distortion coefficient

References

1. Stanford, J. S., ed., Proc. High-Power Laser Optical Components Meeting: 1978, Document NWC-TP-6111 (Naval Weapons Center, China Lake, June '79). Stanford, J. S., ed., Proc. High-Power Laser Optical Components Meeting: 1979, Document NWC-TP-6178 (Naval Weapons Center, China Lake, Aug. '80).

2. Avizonis, P. V., O'Neil, B. D., and Hedin, V. A., "Intensity Mapping Optical Aberrations," Applied Optics, vol. 17 (1978), pp. 1527-31.

3. Bennett, H. E., "Thermal Distortion Thresholds for Optical Trains Handling High Pulse Powers," in Laser-Induced Damage in Optical Materials: 1976 (NBS Special Publication 462, Washington, D.C., Dec. '76), pp. 11-24.

4. Holt, T., "Trade Study of Parameters Influencing High-Spatial-Frequency Distortion in Water-Cooled Mirrors," in Proc. High-Power Laser Optical Components Meeting: 1979 (NWC-TP-6178-Pt. 2, China Lake, Aug. '80), pp. 116-31.

5. Born, M. and Wolf, E., Principles of Optics: Fifth Edition (Pergamon Press, New York, 1975), Chap. 9.

6. Spawr, W. L. and Pierce, R. L., Metal Mirror Selection Guide, Document SOR-74-004 (Spawr Optical Research, Corona, Calif., May '76). Denny, C., Spawr, W., and Pierce, R., "Metal Mirror Selection Guide Update," Proc. SPIE, vol. 181 (1979), pp. 84-9.

7. Sparks, M., "Optical Distortion and Failure in High-Power Reflectors," in Theoretical Studies of High-Power Ultraviolet and Infrared Materials: Eighth-Technical Report(Xonics, Inc., Santa Monica, Dec. '76), pp. 6-153.

8. Carslaw, H. S. and Jaeger, J. C., Conduction of Heat in Solids: Second Edition (Oxford University Press, Oxford, U. K., 1959), Chap. 3.

9. Boley, B. A. and Weiner, J. H., Theory of Thermal Stresses (J. Wiley Inc., New York, 1960), Chap. 9.

10. Klein, C. A., "Mirrors and Windows in Power Optics, "Proc. SPIE, vol. 216 (1980), pp. 204-214.

11. Apollonov, V. V., Bystrov, P. I., Goncharov, V. F., Prokhorov, A. M., and Khomich, V. Y., "Prospects for the Use of Porous Structures for Cooling Power Optics Components," Soviet J. Quantum Electronics, vol. 9 (1979), pp. 1499-505.

12. Gaumer, W., Dichtl, R., and Bloomer, R., "User's Guide to High-Power Mirrors," J. Defense Research, vol. 7B (1975), pp. 249-58.

13. Porteus, J. O., Choyke, W. J., and Hoffman, R. A., "Pulsed Laser Damage Characteristics of Vapor-Deposited Copper Mirrors on Silicon Carbide Substrates," Applied Optics, vol. 19 (1980), pp. 451-4.